Available online at www.sciencedirect.com
SCIENCE DIRECT
Biochemical Pharmacology 67 (2004) 1917–1926
Biochemical Pharmacology
www.elsevier.com/locate/biochempharm

Cloning and characterization of mouse nucleoside triphosphate diphosphohydrolase-3

Élise G. Lavoie, Filip Kukulski, Sébastien A. Lévesque, Joanna Lecka, Jean Sévigny*

Department of Anatomy and Physiology, Centre de recherche en Rhumatologie et Immunologie, Université Laval, Sainte-Foy, Qué., Canada G1V 4G2

Received 2 December 2003; accepted 12 February 2004

Abstract

We have cloned and characterized the nucleoside triphosphate diphosphohydrolase-3 (NTPDase3) from mouse spleen. Analysis of cDNA shows an open reading frame of 1587 base pairs encoding a protein of 529 amino acids with a predicted molecular mass of 58 953 Da and an estimated isoelectric point of 5.78. The translated amino acid sequence shows the presence of two transmembrane domains, eight potential *N*-glycosylation sites and the five apyrase conserved regions. The genomic sequence is located on chromosome 9F4 and is comprised of 11 exons. Intact COS-7 cells transfected with an expression vector containing the coding sequence for mouse NTPDase3 hydrolyzed P2 receptor agonists (ATP, UTP, ADP and UDP) but not AMP. NTPDase3 required divalent cations ($Ca^{2+} > Mg^{2+}$) for enzymatic activity. Interestingly, the enzyme had two optimum pHs for ATPase activity (pH 5.0 and 7.4) and one for ADPase activity (pH 8.0). Consequently, the ATP/ADP and UTP/UDP hydrolysis ratios were two to four folds higher at pH 5.0 than at pH 7.4, for both, intact cells and protein extracts. At pH 7.4 mouse NTPDase3 hydrolyzed ATP, UTP, ADP and UDP according to Michaelis–Menten kinetics with apparent K_ms of 11, 10, 19 and 27 μM, respectively. In agreement with the K_m values, the pattern of triphosphonucleoside hydrolysis showed a transient accumulation of the corresponding diphosphonucleoside and similar affinity for uracil and adenine nucleotides. NTPDase3 hydrolyzes nucleotides in a distinct manner than other plasma membrane bound NTPDases that may be relevant for the fine tuning of the concentration of P2 receptor agonists.

Keywords: NTPDase3; ecto-ATPase; CD39L3; P2 receptors; ATP; UTP

1. Introduction

Ecto-nucleoside triphosphate diphosphohydrolase (E-NTPDase) designates a family of transmembrane proteins that catalyze the hydrolysis of γ and/or β phosphate residues of nucleotides [1]. Members of this enzyme family possess five characteristic apyrase conserved regions (ACR) [2–4], one or two transmembrane domains and they require divalent cations, such as Ca^{2+} or Mg^{2+}, for their activity [1].

Four members of the family are tightly bound to the plasma membrane via two transmembrane domains, and have a large extracellular region with an active site facing the extracellular milieu. These enzymes hydrolyze nucleoside triphosphates (e.g. ATP) and diphosphates (e.g. ADP) with different ability. NTPDase1 (CD39) [5,6] hydrolyzes both ATP and ADP equally well whereas NTPDase2 (CD39L1) [7,8] prefers triphosphonucleosides. NTPDase3 (also named CD39L3 and HB6 [9,10]) and NTPDase8 [11] slightly prefer ATP over ADP by a ratio of about 3 and 2, respectively. Other members of the E-NTPDase family are associated with membranes of intracellular organelles (NTPDases 4–7) and have different particularities regarding, for example, substrate specificity and membrane topology. NTPDase4 (hLALP70) [12–14] prefers UDP as substrate and is anchored by two transmembrane domains in the Golgi apparatus. NTPDase5 (CD39L4) [15] and NTPDase6 (CD39L2) [16–18] have a preference for nucleoside diphosphates and possess a single transmembrane domain near the N-terminus of the protein. The first is bound to the endoplasmic reticulum and the second to the Golgi apparatus. A soluble form of the two latter

Abbreviations: ACR, apyrase conserved region; EST, expressed sequence tag; NTPDase, nucleoside triphosphate diphosphohydrolase; RT, reverse transcription

* Corresponding author. Tel.: +1-418-654-2772; fax: +1-418-654-2765.
E-mail address: Jean.Sevigny@crchul.ulaval.ca (J. Sévigny).

0006-2952/$ – see front matter © 2004 Elsevier Inc. All rights reserved.
doi:10.1016/j.bcp.2004.02.012

enzymes can be secreted after a proteolytic cleavage. Finally, NTPDase7 (LALP1) [19], prefers nucleoside triphosphates as substrates and is located in intracellular vesicles.

Our laboratory studies the function of plasma membrane bound NTPDases (members 1–3 and 8) using mouse models. NTPDases 1, 2 and 8 have been cloned in human and mouse while NTPDase3 has been cloned in human [9] and recently in rat (personal communication from Dr. H. Zimmermann). NTPDase3 (HB6) cDNA was originally cloned from a human brain library [9]. Northern Blots show strong expression of human NTPDase3 in brain, pancreas, spleen and prostate, and weak expression in a few other tissues [10]. Rat NTPDase3 mRNA was found by RT-PCR in PC12, a rat neural cell line [20]. The human form has a molecular mass of 79 kDa with seven potential *N*-glycosylation sites that are important for enzymatic activity [21], especially the site near ACR1 [22]. Dr. Kirley's group in Cincinnati has demonstrated by directed mutagenesis that the substitution of various amino acid residues of human NTPDase3 abrogated phosphohydrolase activity and/or affected substrate specificity [23–26]. They have documented the relationship between the active site of NTPDases with the nucleotide binding site of actin/heat shock 70/sugar kinase superfamily [27]. They have also shown that the transmembrane domains of human NTPDase3 play a role in the formation of the quaternary structure of the protein, which would be constituted by an asymmetric dimer of dimers linked by a disulfide bond between intracellular cysteine residues 10 [28]. In human NTPDase1, the transmembrane domains also regulates enzymatic activity [29] and substrate specificity [30].

This sums up most of the actual knowledge about human NTPDase3. Orthologues from other species have not yet been reported except for data based on ESTs and RT-PCR of a fragment that would be expected to be the homologue of human NTPDase3. These experiments suggested the expression of NTPDase3 in rat [20] and mouse [10]. In this work we have cloned NTPDase3 from mouse spleen and have characterized its biochemical properties related to the regulation of the concentration of P2 receptor agonists.

2. Materials and methods

2.1. Materials

Agarose, aprotinin, ethylenediaminetetraacetic acid (EDTA), ethylene glycol-bis(2-aminoethylether)-*N*-*N*-*N*′-*N*′-tetraacetic acid (EGTA), sodium acetate, 2-(4-morpholino)-ethane sulfonic acid (MES), nucleotides, phenylmethylsulfonyl fluoride (PMSF), sodium acetate, tetrabutylammonium hydrogen sulphate (TBA) and Tris(hydroxymethyl) aminomethane (Tris) were purchased from Sigma-Aldrich. All cell culture media were obtained from Invitrogen and 24-well plates from VWR Canlab.

2.2. RT-PCR cloning

Total RNA was isolated from mouse spleen with Trizol reagent (Invitrogen). cDNA was synthesized with SuperScript II (Invitrogen) from 500 ng of total RNA with oligo $(dT)_{18}$ as the primer, in accordance with manufacturer's instructions (Invitrogen). For amplification, 10% of the reverse transcription (RT) reaction was used as template in a final volume of 50 μl reaction mixture containing 0.6 μM primer, 400 μM dNTP and 3.5 U Expand High Fidelity PCR System (Roche). The following set of primers were designed based on the 5′ and 3′ ends of EST sequences (GenBank accession numbers BB644796 and W46136, respectively): forward 5′CTT-TTC-AGC-AAC-CCG-CAG-C3′, reverse 5′TTC-CTG-CCA-GAG-CAC-CTC-C3′. Amplification was started with 2 min 30 s at 94 °C followed by 35 cycles of 30 s denaturation at 94 °C, 1 min annealing at 62 °C, 2 min primer extension at 72 °C and ended by 7 min incubation at 72 °C. The PCR product of approximately 1.8 kb was purified on agarose gel using the QIAEX II gel extraction kit (Qiagen) and ligated into the expression vector pcDNA3.1/V5-His (Invitrogen). Plasmid DNA was purified with QIAprep Spin Miniprep kit (Qiagen) and orientation of the insert verified by restriction mapping. Two independent fragments cloned from different PCR reactions were amplified and fully sequenced in one direction. The sequences of both clones were identical.

2.3. Genomic characterization of Entpd3

The obtained mouse NTPDase3 cDNA sequence was used to search the National Center for Biotechnology Information (NCBI) mouse genome database. The sequence identified as NT_039482 revealed perfect identity. The exon/intron junctions and their characteristics were analyzed with NCBI BLAST programs.

2.4. COS-7 cell transfection and protein preparation

COS-7 cells were transfected in 10 cm plates using Lipofectamine (Invitrogen), as previously described [6]. Briefly, 60–80% confluent cells were incubated for 5 h at 37 °C in DMEM in absence of fetal bovine serum (FBS) with 6 μg of plasmid DNA and 24 μl of Lipofectamine reagent. Then, an equal volume of DMEM containing 20% FBS was added and 40–44 h later cells were collected for analysis. For protein preparation, transfected cells were washed three times with Tris–saline buffer at 4 °C, harvested by scraping in 95 mM NaCl, 0.1 mM PMSF and 45 mM Tris, pH 7.5, and washed twice by centrifugation at 300 × *g* for 5 min at 4 °C. Cells were resuspended in the harvesting buffer containing 10 μg/ml aprotinin and sonicated. Nuclear and cellular debris were discarded after another centrifugation as described above, and resulting supernatant was kept at −80 °C until use. Protein concentration was estimated by the Bradford microplate assay,

using bovine serum albumin as a standard of reference [31].

2.5. NTPDase activity measurement

The protein extract's enzyme activity was measured at 37 °C in 0.5 ml of the following incubation medium: 5 mM $CaCl_2$, 80 mM Tris, pH 7.4 as described previously [32]. Enzyme preparation was added to the incubation mixture and pre-incubated for 3 min. Unless indicated otherwise, reaction was started with 0.5 mM substrate (ATP, ADP, UTP, UDP or AMP), stopped after 20 min by the addition of 0.125 ml of malachite green reagent, and the inorganic phosphate released during the hydrolysis of the exogenous nucleotide measured [33]. The biochemical activities at the surface of intact COS-7 cells transiently transfected with NTPDase3 expression vector were evaluated in 24-well plates. Activity assays were carried out in similar conditions with the addition of 145 mM NaCl to the incubation medium and stopped by sampling an aliquot of 0.2 ml and rapid mixing with 50 μl of malachite green reagent. Optimum pH was determined using the following buffers: 100 mM acetate for pH 4.0–5.5, 100 mM MES for pH 5.5–7.0 or 100 mM Tris for pH 7.0–9.0, in the presence of 5 mM $CaCl_2$. In the indicated experiments $MgCl_2$ replaced $CaCl_2$, and for controls, 1 mM EDTA plus 1 mM EGTA were added instead of divalent cation to chelate residual Mg^{2+} and Ca^{2+}. All experiments were performed in triplicate with appropriate controls.

2.6. Separation and quantification of nucleotides by HPLC

Enzymatic reaction was carried out as described above. Aliquots of 20 μl from the reaction mixture were taken at specific time points and transferred to a fresh tube containing an equal volume of ice-cold 1 M perchloric acid. The samples were centrifuged for 5 min at 1000 × *g*. Supernatants were neutralized with 1 M KOH (4 °C), centrifuged for 5 min at 1000 × *g* and then lipids were removed by liquid-liquid extraction with *n*-heptane (5:1, v/v). The nucleotide content of the samples was determined in 20 μl aliquots separated by HPLC-RP under isocratic conditions.

Adenine nucleotides (ATP, ADP and AMP) were separated on a 15 cm × 4.6 mm, 3 μm SUPELCOSIL™ LC-18-T column (Supelco) with a mobile phase composed of 25 mM TBA, 5 mM EDTA, 100 mM KH_2PO_4/K_2HPO_4, pH 7.0 and 2% (v/v) methanol, at a flow-rate of 1 ml/min. Uracil nucleotides (UTP, UDP and UMP) were resolved using SUPELCOSIL™ LC-18-T column (25 cm × 4.6 mm, 5 μm, Supelco) as described above with the difference that the mobile phase did not contain methanol. Combined adenine and uracil nucleotide samples were analyzed with the latter column and a mobile phase composed of 16.7 mM TBA, 3.3 mM EDTA, 66.7 mM KH_2PO_4/K_2HPO_4, pH 7.0. The flow rate was 0.5 ml/min for the first 20 min and then 1 ml/min up to 90 min. The nucleotides were detected by UV absorption at 260 nm and identified by comparison with retention time and UV spectrum of the appropriate standards.

3. Results

3.1. Cloning and nucleic acid analysis of mouse NTPDase3 cDNA

Mouse NTPDase3 cDNA was cloned by RT-PCR with oligonucleotide primers designed from potential EST sequences selected from a homology search with the human cDNA sequence. The nucleic acid sequences of the two independent clones obtained were identical. They showed an open reading frame (ORF) of 1587 bp encoding a protein of 529 amino acid residues with a predicted molecular mass of 58 953.5 Da and an isoelectric point of 5.78. The deduced amino acid sequence reveals the five ACRs, eight potential *N*-glycosylation sites, putative phosphorylation sites on the extracellular loop and one protein kinase C consensus phosphorylation site in the intracellular C-terminal segment at residue 511 (Fig. 1 and data not shown). Hydropathicity analysis of mouse NTPDase3 amino acid sequence predicted the presence of two transmembrane domains, one at the N terminus between the amino acid residues 21 and 43 and one at the C terminus between residues 486 and 508 (Fig. 2). The amino acid sequence alignment of 18 members of the E-NTPDase family and related proteins with mouse NTPDase3 was generated with GeneBee software (http://www.genebee.msu.su/). As expected, the highest homology was found with rat NTPDase3 (94.3%), recently added to the data base, and human NTPDase3 (81.3%; Fig. 3).

3.2. Genomic characterization of Entpd3

A homology search in the Mouse Sequence Data Base (www.ncbi.nih.gov/genome/seq/MmBlast.html) with NTPDase3 cDNA located the gene to chromosome 9F4 (entry NT_039482). Alignment of the cDNA sequence with the mouse genomic sequence reveals that the gene covers over 26.9 kb and is organized into 11 exons and 10 introns, all in agreement with the donor/acceptor rule. The precise length of the first (non-coding) exon as well as three introns can not be measured at the moment (Table 1). Fig. 4 and Table 1 summarize the genomic structure of mouse *Entpd3*.

3.3. Biochemical characterization of mouse NTPDase3

The biochemical characteristics of mouse NTPDase3 were determined with crude protein extracts, and/or with intact COS-7 cells transiently transfected with pcDNA3.1/V5-His containing mouse NTPDase3 cDNA. The time

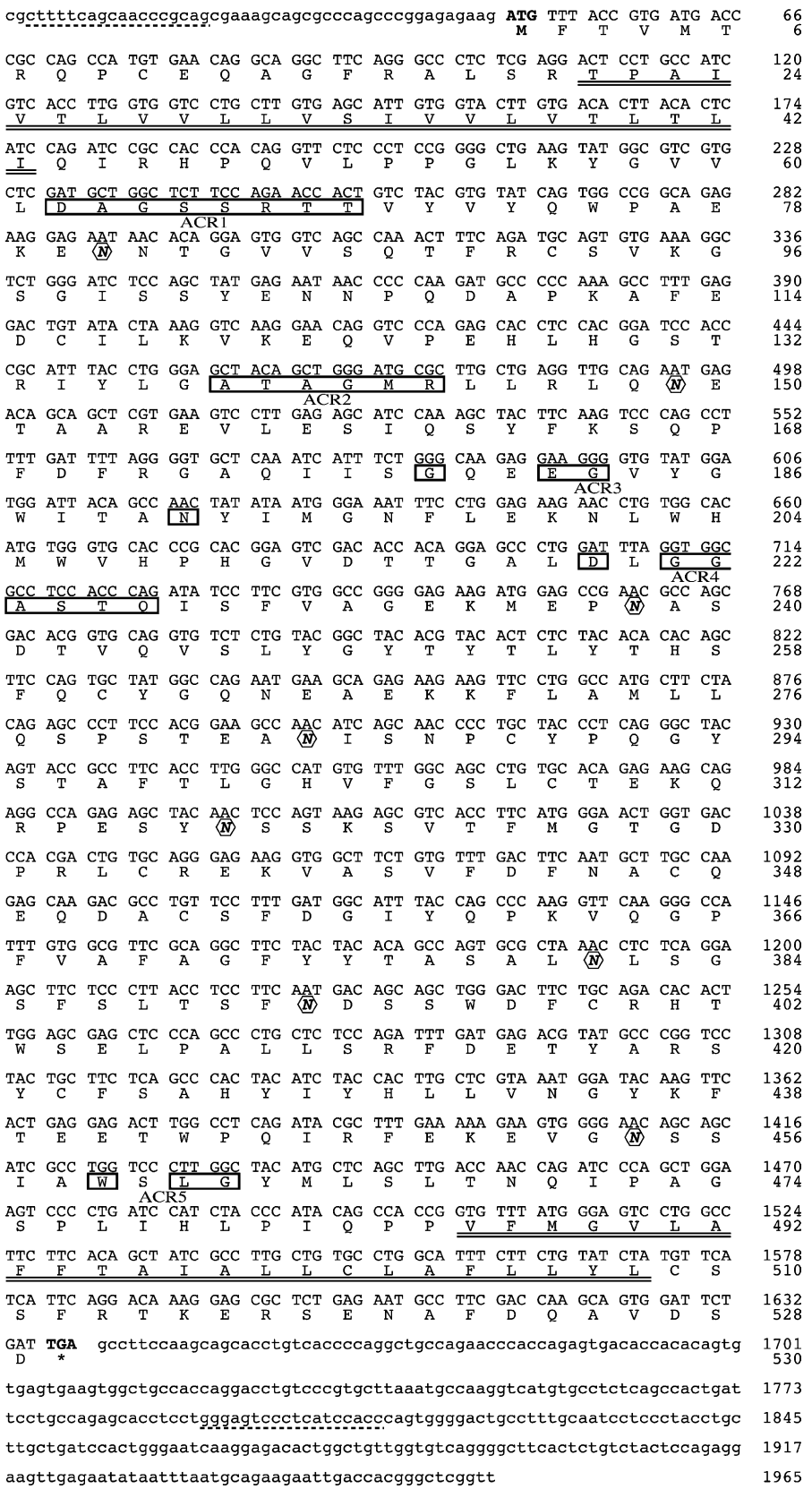

Fig. 1. Nucleotide and predicted amino acid sequence of mouse NTPDase3 cDNA. The initiation codon and stop codon (indicated by ∗) are bold face, potential *N*-glycosylation sites are represented by "*N*" surrounded by an hexagon, two hydrophobic regions are double underlined and the five apyrase conserved regions (ACR 1–5) are boxed. The two oligonucleotide primers used for PCR are indicated by dotted lines and the 5′ (1–2) and 3′ (1810–1965) non-coding sections presented were obtained from mouse EST sequences, GeneBank accession number BB644796 and W46136, respectively.

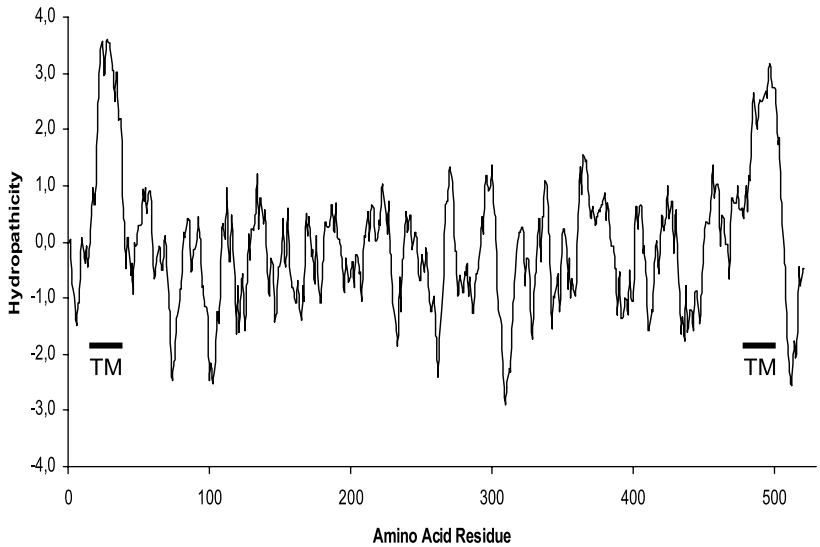

Fig. 2. Hydropathicity analysis of mouse NTPDase3. The deduced amino acid sequence was analyzed according to the method of Kyte and Doolittle [39]. Bars indicate the two predicted transmembrane domains (TM) corresponding to amino acids 21–43 and 486–508.

course study with protein extracts revealed that the reaction was linear for the first 60 min with either ATP or ADP as substrate (Fig. 5A). The following assays were carried out for 15–20 min. Murine NTPDase3 required divalent cations for enzymatic activity, Ca^{2+} being more effective than Mg^{2+} as tested for ATP and ADP (Fig. 5B). In the presence of 1 mM EDTA and 1 mM EGTA, to remove traces of divalent cations, no activity could be detected (Fig. 5B). Fig. 5C shows that ATPase activity of NTPDase3 had two maxima, one at pH 5.0 and a second at pH 7.4. In contrast, using the plasmids kindly provided by Dr. Kirley and Dr. Zimmerman, a single maximum was observed at physiological pH for both the human and rat orthologues (data not shown). With ADP as substrate, the biochemical activity was relatively similar between pH 5.5 and 9.0 with a maximal activity at pH 8.0 that was statistically sig-

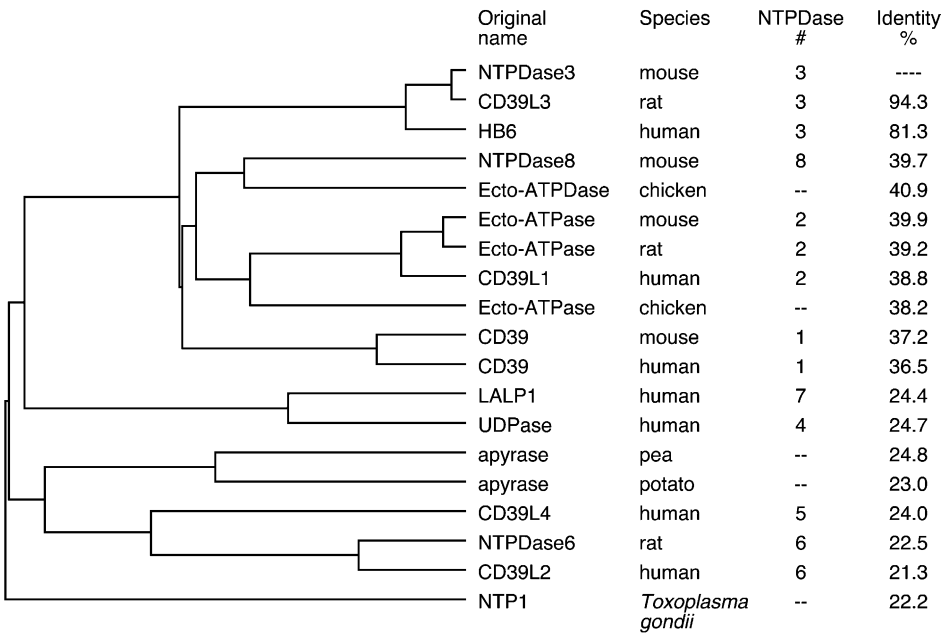

Fig. 3. Phylogenetic analysis of amino acid sequences of selected NTPDases and related proteins. The percentage of amino-acid identity of these proteins with mouse NTPDase3 was determined by pairwise alignment using ALIGN*p* (http://www.infobiogen.fr/services/analyseq/cgi-bin/alignp_in.pl). The GeneBank accession numbers of the sequences are as follows: mouse NTPDase3, AY376710; rat CD39L3, NM_178106; human HB6, AF034840; chicken ecto-ATPDase, AF041355; mouse NTPDase8, AY364442; mouse NTPDase2, AY376711; rat ecto-ATPase, Y11835; human CD39L1, NM_001246; chicken ecto-ATPase, U74467; mouse CD39, AF037366; human CD39, S73813; human LALP1, AF269255; human UDPase, AF016032; pea apyrase, Z32743; potato apyrase, U58597; human CD39L4, AF039918; rat NTPDase6, AJ277748; human CD39L2, AF039916; *Toxoplasma gondii* apyrase, U96965.

Table 1
Summary of the genomic structure of mouse *Entpd3*

Exon	Position in NT_039482.2	Splice acceptor	Length of exon (bases)	Splice donor	Length of intron (bases)	Nucleotide position of important sequences in current exon
1	10888830–10888855	na	>66	AGCGCCCAG/gtaaggtct	768	Promoter −227 to −150
2	10889624–10889675	cccctgcag/CCCGGAGAG	52 (from Met 40)	AACAGGCAG/gtaagtgtt	≥3344	Met 13–15
3	10893020–10893147	tcattgcag/GCTTCAGGG	128	GGGCTGAAG/gtaagccgg	≥10 248	
4	10903396–10903513	tccctgcag/TATGGCGTC	118	GTGTGAAAG/gtaaagggg	≥1303	ACR1* 16–39
5	10904817–10904967	gctcttcag/GCTCTGGGA	151	CTTGCTGAG/gtaagggct	1596	ACR2 126–143
6	10906564–10906723	cttgcatag/GTTGCAGAA	160	TTCCTGGAG/gtgtgtgga	784	ACR3 98–136
7	10907508–10907741	actatgcag/AAGAACCTG	234	CTTCTACAG/gtaccaggg	1911	ACR4 58–81
8	10909653–10909925	tacctccag/AGCCCTTCC	273	CCATTTGTG/gtaagaggc	167	
9	10910093–10910203	cgctcacag/GCGTTCGCA	111	TGGAGCGAG/gtcagtatt	867	
10	10911071–10911208	cctttccag/CTCCCAGCC	138	GAAAAAGAA/gtaagtgca	4269	
11	10915478–10915711	cctccacag/GTGGGGAAC	Up to TGA 234	TGA		ACR5 22–33 TGA 235-237
					Introns + exons >26 922	polyA 1187 bp after TGA

Sizes and junctions of the exons and introns of mouse *Entpd3* are presented according to the sequence of accession No. NT_039482.2. Intron sequences are given in small characters and exons in capitals. As the gene has not been fully sequenced yet the length of the introns between exons 2–3, 3–4 and 4–5 can not be measured with precision at this point.

* ACR: Apyrase conserved region; na: not available.

nificant ($P < 0.01$). The specificity of substrate for calcium dependent ecto-nucleotidase activity on intact transiently transfected COS-7 cells is illustrated on Fig. 5D for the two pHs that showed the highest ATPase activity (Fig. 5C). Mouse NTPDase3 hydrolyzed all triphospho- and diphosphonucleosides tested with a preference for triphosphonucleosides. As with all other NTPDases, this enzyme did not hydrolyze AMP (Fig. 5D). Interestingly, the NTP/NDP hydrolysis ratio changed with pH. At pH 7.4 the hydrolysis ratios measured with intact transfected cells were 2.7 ± 0.8 (mean ± S.D.) and 5.4 ± 1.6 for ATP/ADP and UTP/UDP, respectively. These ratios were significantly increased to 3.6 ± 0.9 and 14.5 ± 5.4 at pH 5.0 with P values <0.001. With protein extracts, the ATPase and UTPase activities were two fold higher at pH 5.0 compared to pH 7.4, making a slightly more pronounced change between the hydrolysis ratios at these two pHs (Fig. 5C and data not shown). These higher ATPase and UTPase activities at pH 5.0 with protein extracts, when compared to the activity measured on intact transiently tranfected cells, were observed in all experiments. This may be attributable to the contribution of newly synthesized and immature NTPDase3 in the protein extracts.

To confirm the tight association of mouse NTPDase3 to a membrane fraction, we performed an ultracentrifugation of the protein extract at 100 000 × g for 1 h. Over 87% of ATPase and ADPase activities were found in the pellet (data not shown). The above observation, together with the fact that biochemical activity was detected at the cell surface of NTPDase3 transfected COS-7 cells, confirmed that mouse NTPDase3 is an ectoenzyme tightly bound to the plasma membrane.

3.4. Kinetics of mouse NTPDase3

The kinetic parameters for the substrates that are also the agonists of P2 receptors were evaluated. Plotting the initial velocities as a function of substrate concentration resulted in a typical hyperbolic curve of the Michaelis–Menten model (Fig. 6A for UTP and data not shown for UDP, ATP and ADP). The apparent kinetic constants were evaluated using the method of Woolf–Augustinsson–Hofstee and are summarized in Table 2. The comparison of apparent K_m values showed that ATP and UTP had two times higher affinity for the enzyme compared to their respective diphosphonucleoside (Table 2 and Fig. 6A).

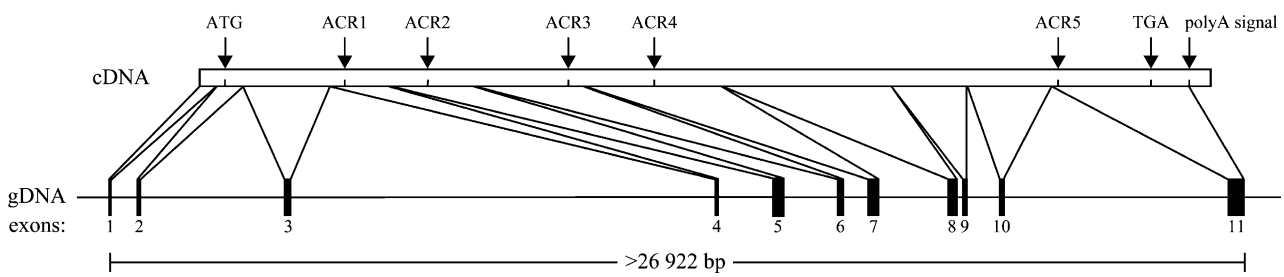

Fig. 4. Schematic representation of the genomic organization of mouse *Entpd3*. The gene contains 11 exons spanning over 26.9 kb on mouse chromosome 9 band F4. Start and stop codons, ACRs 1–5 as well as polyA signal are indicated on the cDNA. Exons are presented by black boxes on the genomic DNA (gDNA). Further information is given in Table 1.

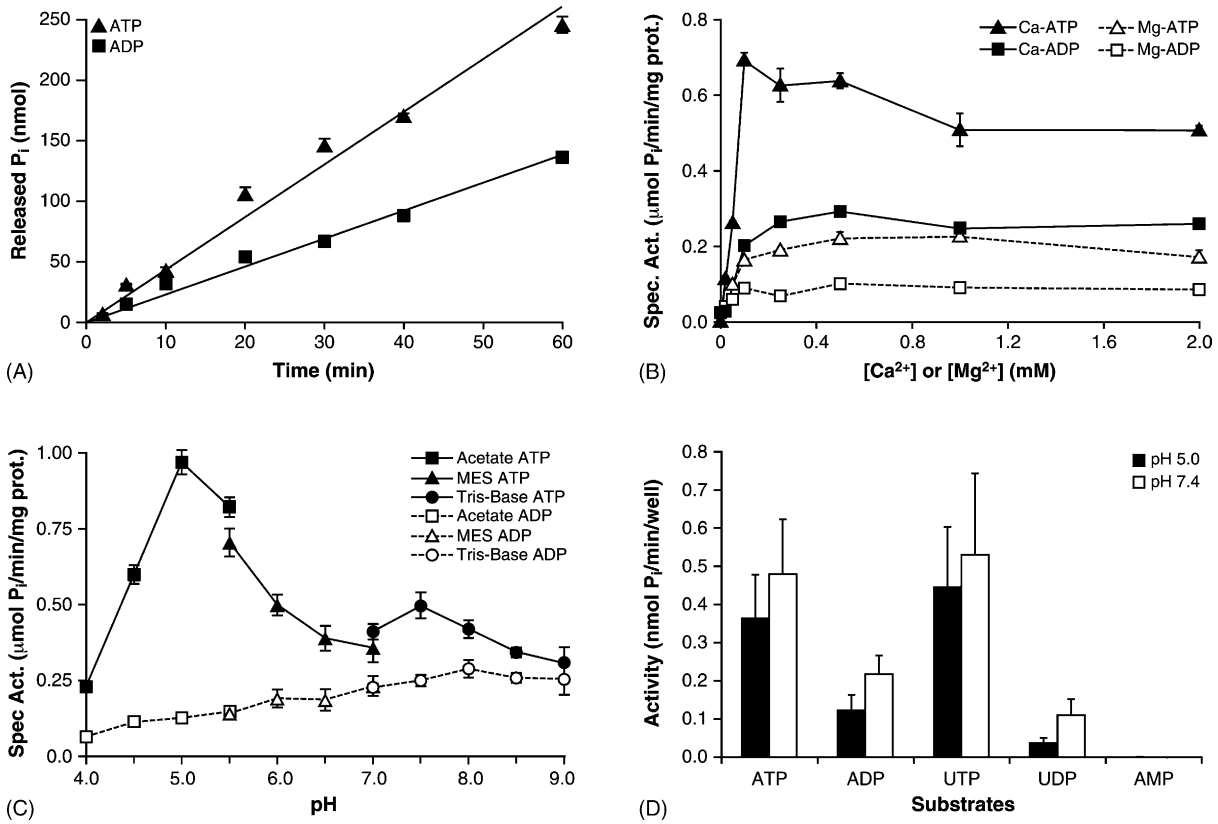

Fig. 5. Biochemical characterization of mouse NTPDase3. Enzyme activity assays of protein extracts from NTPDase3 transfected COS-7 cells were carried out in 5 mM $CaCl_2$, 0.5 mM nucleotides, 100 mM Tris, pH 7.4 unless stated otherwise (panels A and C). For intact cells 145 mM NaCl was added to the incubation medium (panel D). In these experiments, less than 5% of the substrate was hydrolyzed. ATPase and ADPase activities were assayed. For panel A, a representative experiment out of two independent experiments is shown and for panels B–D, results are expressed as the mean ± S.D. of two to five independent experiments. Each individual experiment was performed in triplicate. (A) Time course of ATP and ADP hydrolysis by NTPDase3. Linear regression gave a similar r^2 of 0.98 for both ATP and ADP. (B) Effect of calcium (Ca^{2+}) and magnesium (Mg^{2+}) ions. NTPDase3 was more active in the presence of Ca^{2+} (solid symbols and full lines) than in presence of Mg^{2+} (open symbols and dotted lines) with the ATPase (▲) activity being higher then ADPase (■) activity for both cations. (C) Effect of pH. Three different buffers were used: acetate: pH 4.0–5.5 (■); MES: pH 5.5–7.0 (▲); Tris: pH 7.0–9.0 (●), solid symbols and full lines for ATP and open symbols and dotted lines for ADP. Activities for both ATP (at pHs 5.0 and 7.4) and ADP (at pH 8.0) were significantly higher than the activities measured at the surrounding pHs ($P < 0.01$). (D) Substrate specificity of NTPDase3 expressed at the surface of intact transiently transfected cells at pH 5.0 (filled bars) and 7.4 (open bars).

HPLC analysis of ATP and UTP hydrolysis by protein extracts from NTPDase3 expressing COS-7 cells showed a transient accumulation of the corresponding diphosphonucleoside (ADP or UDP; Fig. 6B and C). Similar data were observed with intact transfected cells (data not shown). Finally, when ATP and UTP were added together to the incubation medium, similar rates of hydrolysis were observed for both adenine and uracil nucleotides (Fig. 6D).

4. Discussion

This work describes the cloning and biochemical characterization of mouse NTPDase3. The genomic localization of mouse *Entpd3* on locus 9F4 confirmed that the protein expressed is distinct from other NTPDases. The human orthologue is located on chromosome 3 [10], the homologous region to mouse chromosome 9. Mouse *Entpd3,* as for *ENTPD3*, is comprised of 11 exons (Fig. 4 and data not shown). The open reading frame of its cDNA reveals the presence of 529 amino acid residues as for human (HB6) [9] and rat (sequence recently added to the database) orthologues (Fig. 1 and data not shown). The amino acid identity of mouse NTPDase3 with these two proteins is over 80% (Fig. 3). Various sites are conserved between these three enzymes including *N*-glycosylation and putative phosphorylation sites. The potential *N*-glycosylation sites are all conserved with the exception that mouse NTPDase3 has an additional potential site on residue 318 (Fig. 1). Protein glycosylation is important for the catalytic activity of human NTPDase3 [21], especially on asparagine 81 near ACR1 [22]. The analysis of the amino acid sequence of these proteins reveals a putative protein kinase C phosphorylation site in the C-terminal segment of mouse NTPDase3 (serine 511), and on HB6 (serine 512) [9]. The rat orthologue does not possess any phosphorylation site in the intracellular portion of the protein. A protein kinase C phosphorylation site is also present in the intracellular domain of other plasma membrane bound NTPDases: human [7] and mouse NTPDase2

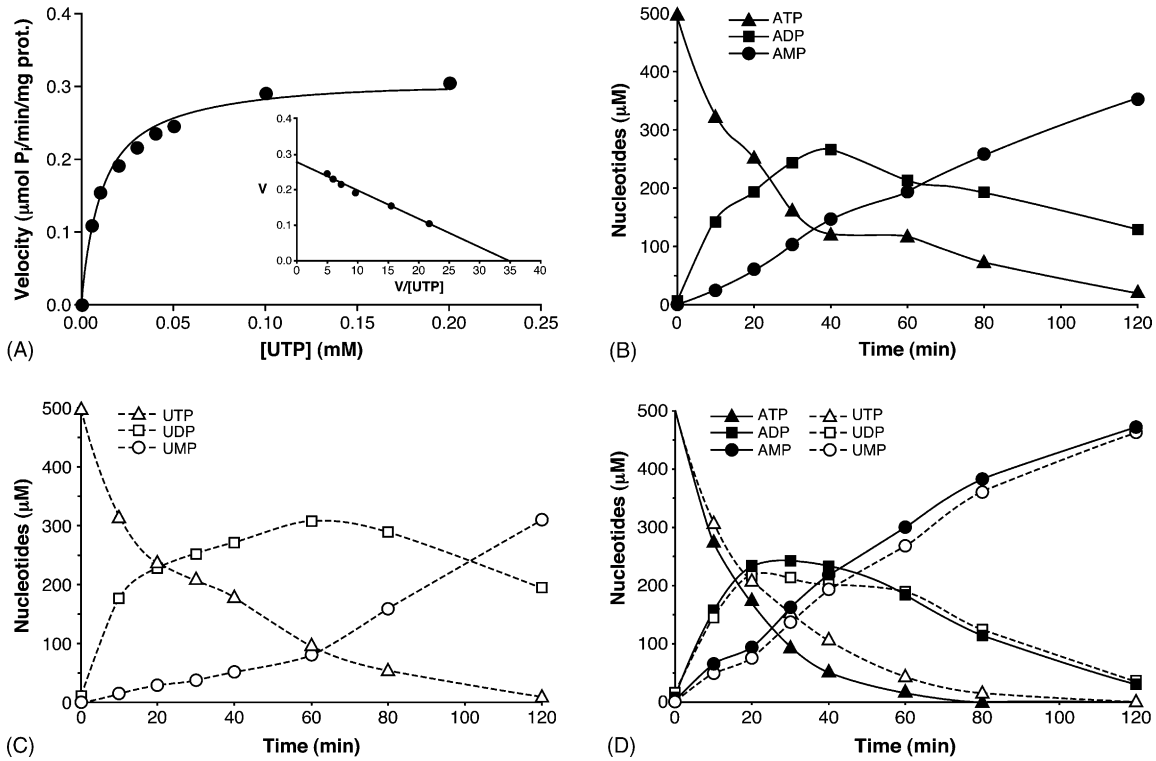

Fig. 6. Kinetics and profile of nucleotides hydrolysis by mouse NTPDase3. For panel A, reaction was carried out for 12 min in the presence of 5 mM $CaCl_2$ and 100 mM Tris pH 7.4. The average of three separate experiments each performed in triplicate is presented. Graphs were produced using GraphPad Prism software (GraphPad Software Inc.). For the analysis of ATP and UTP hydrolysis products (panels B and C), the reaction was started by the addition of 32 µg of NTPDase3 protein extract to the reaction mixture containing 0.5 mM substrate. For the analysis of the combined dephosphorylation of ATP and UTP (panel D), the reaction was initiated with 78 µg of protein extract. Aliquots were taken at different time points and reaction stopped by the addition of an equal volume of ice-cold 1 M perchloric acid. These samples were deproteinated, lipids removed and the nucleotide content analyzed by HPLC as described in Section 2. (A) Michaelis–Menten representation of the hydrolysis of UTP with concentrations ranging from 5 to 200 µM. Inset, Woolf–Augustinsson–Hofstee plot was used to evaluate the apparent K_m and V_{max} using the points in the linear portion of the curve in the Michaelis–Menten representation (5–50 µM). The kinetic parameters are presented in Table 2. (B) Nucleotide content of samples collected at different time points of ATP hydrolysis by murine NTPDase3 protein extracts: ATP (▲), ADP (■), AMP (●). (C) UTP hydrolysis by NTPDase3 protein extracts: UTP (△), UDP (□), UMP (○). (D) Simultaneous hydrolysis of ATP and UTP by NTPDase3: ATP (▲), ADP (■), AMP (●), UTP (△), UDP (□), UMP (○).

have one in the C-terminal portion (serine 488), whereas human and mouse NTPDase8 possess one in the N-terminal portion (serine 4) [11]. Whether phosphorylation plays a role in NTPDase functions is not known.

We observed that mouse NTPDase3 was tightly associated with the plasma membrane with an active site facing the extracellular milieu. The highest homology of this protein was observed with the other NTPDases bearing the same characteristics: mammalian NTPDases 1, 2 and 8 and the two related proteins from chicken described as an ATPase [34] and an ATPDase [35] (Fig. 3). The biochemical characteristics of NTPDases 1 and 2 have been largely documented while NTPDase8 has been identified only recently [11]. Similar to NTPDase1 and 8, but in contrast to NTPDase2, NTPDase3 prefers Ca^{2+} over Mg^{2+} for both ATPase and ADPase activities (Fig. 5B). One of the particularities of mouse NTPDase3 is a biphasic curve for ATPase activity as a function of pH with a first maximum at pH 5.0 and a second at 7.4 (Fig. 5C). In comparison, the optimal pH of human and rat orthologues showed a single maximum at pH 7.5 for ATPase activity (data not shown). Whether this reflects some variation in the amino acid composition of the catalytic site remains to be elucidated. Interestingly, mouse NTPDase3 had only one peak of activity at pH 8 with ADP as substrate. Consequently, this characteristic affected the ATP/ADP and UTP/UDP hydrolysis ratios, which were increased by two to four folds between physiological to acidic pHs. At more alkaline pHs the ATP/ADP hydrolysis ratio was close to 1 for protein extracts (Fig. 5C). This may affect the control of extracellular nucleotide levels according to the pH and location of the enzyme.

Table 2
Kinetic parameters of mouse NTPDase3

Substrate	K_m (µM)	V_{max} (U/mg of protein)
ATP	11 ± 2	0.35 ± 0.02
UTP	10 ± 1	0.30 ± 0.01
ADP	19 ± 2	0.22 ± 0.01
UDP	27 ± 2	0.14 ± 0.01

K_m and V_{max} values were estimated by regression analysis of Woolf–Augustinsson–Hofstee plots. Results are expressed as the mean ± S.E.M. The curves drawn from these data gave an r^2 of 0.97, 0.99, 0.98 and 0.99 for ATP, UTP, ADP and UDP, respectively.

The hydrolysis of ATP and UTP by mouse NTPDase3 showed a transient accumulation of the corresponding diphosphonucleoside (ADP and/or UDP). When the level of triphosphonucleoside(s) had sufficiently decreased, then AMP or UMP accumulated in the medium (Fig. 6B and D). This is in agreement with the measured kinetic constants of mouse NTPDase3. The apparent K_m for ATP and UTP were half as much as the corresponding diphosphonucleoside (Table 2). In comparison, NTPDase1 hydrolyzes ATP to AMP, one P_i at a time, without any accumulation of ADP. In contrast, NTPDase2 hydrolyzes preferentially ATP to ADP, the latter being a poor substrate of the enzyme. The pattern of hydrolysis of NTPDase3 is somewhat in between the one of NTPDase1 and NTPDase2 [8]. For NTPDase1, the apparent K_ms are similar for ATP and ADP, in the order of 10 μM [36,37]. For human NTPDases 2 and 3 these constants are in the high micromolar range. Hence, for intact NIH-3T3 cells stably transfected with NTPDase2, the apparent K_ms were around 400 μM for ATP and 100 μM for ADP with apparent V_{max}s of 107 and of 4 nmol P_i/min per 10^6 cells, respectively [7]. The apparent K_ms of human NTPDase3 for ATP and ADP, evaluated from protein extracts of transiently transfected COS-1 cells, were 128 and 96 μM, respectively, with apparent V_{max}s of 2.0 and 0.5 μmol P_i/min/mg of protein [27].

The plasma membrane bound NTPDases 1–3 and 8 control the nucleotide levels in extracellular spaces, and therefore, modulate P2 receptor signaling. The difference in the biochemical and kinetic properties of these ectonucleotidases may have profound physiological effects. The affinity of the substrates toward the enzymes, the specific activity and the products formed may determine distinct roles for each plasma membrane bound NTPDase. For example, we have recently shown that the different hydrolysis patterns of NTPDase1 and NTPDase2 dictated their opposing roles in the control of platelet aggregation, as demonstrated in vitro [38]. The AMP generated by NTPDases, can then be further hydrolyzed by the ecto-5′-nucleotidase to adenosine. Thus, the hydrolysis products of ATP (ADP and adenosine) react with different subtypes of P2 and P1 receptors and trigger different physiological actions.

In summary, the distinct biochemical properties of mouse NTPDase3 suggest that it controls extracellular nucleotide levels differently than other ectonucleotidases, including NTPDases 1 and 2, and would therefore regulate P2 receptor activation in a distinctive manner. Future work on the cellular localization and expression pattern of the enzyme shall help define its potential function.

Acknowledgments

We thank Mrs. Julie Pelletier and Mr. François Bigonnesse for their technical assistance. This work was supported by grants from the Canadian Institutes of Health Research (CIHR; MOP-49460 and M2C-50334) and from the ‘‘Fonds de la Recherche en Santé du Québec’’ (FRSQ; 2822) to J.S.

References

[1] Zimmermann H. Ectonucleosides: some recent developments and a note on nomenclature. Drug Dev Res 2001;52:44–56.
[2] Vasconcelos EG, Ferreira ST, de Carvalho TMU, de Souza W, Kettlun AM, Mancilla M, et al. Partial purification of ATP diphosphohydrolase from *Schistosoma mansoni*. J Biol Chem 1996;271:22139–45.
[3] Schulte AM, Esch II J, Sévigny J, Kaczmarek E, Siegel JB, Imai M, et al. Structural elements and limited proteolysis of CD39 influence ATP diphosphohydrolase activity. Biochemistry 1999;38:2248–58.
[4] Handa M, Guidotti G. Purification and cloning of a soluble ATP-diphosphohydrolase (apyrase) from potato tubers (*Solanum tuberosum*). Biochem Biophys Res Commun 1996;218:916–23.
[5] Wang TF, Guidotti G. CD39 is an ecto-(Ca^{2+}, Mg^{2+})-apyrase. J Biol Chem 1996;271:9898–901.
[6] Kaczmarek E, Koziak K, Sévigny J, Siegel JB, Anrather J, Beaudoin AR, Bach FH, Robson SC. Identification and characterization of CD39 vascular ATP diphosphohydrolase. J Biol Chem 1996;271:33116–22.
[7] Mateo J, Harden TK, Boyer JL. Functional expression of a cDNA encoding a human ecto-ATPase. Br J Pharmacol 1999;128:396–402.
[8] Kegel B, Braun N, Heine P, Maliszewski CR, Zimmermann H. An ecto-ATPase and an ecto-ATP diphosphohydrolase are expressed in rat brain. Neuropharmacology 1997;36:1189–200.
[9] Smith TM, Kirley TL. Cloning, sequencing, and expression of a human brain ecto-apyrase related to both the ecto-ATPases and CD39 ecto-apyrases. Biochim Biophys Acta 1998;1386:65–78.
[10] Chadwick BP, Frischauf AM. The CD39-like gene family—identification of three new human members (CD39L2, CD39L3, and CD39L4) their murine homologues, and a member of the gene family from drosophila melanogaster. Genomics 1998;50:357–67.
[11] Bigonnesse F, Lévesque SA, Kukulski F, Lecka J, Robson SC, Fernandes MJG, Sévigny J. Cloning and characterization of mouse nucleoside triphosphate diphosphohydrolase-8. Biochemistry, in press.
[12] Wang TF, Guidotti G. Golgi localization and functional expression of human uridine diphosphatase. J Biol Chem 1998;273:11392–9.
[13] Biederbick A, Rose S, Elsasser HP. A human intracellular apyrase-like protein LALP70, localizes to lysosomal/autophagic vacuoles. J Cell Sci 1999;112:2473–84.
[14] Biederbick A, Kosan C, Kunz J, Elsasser HP. First apyrase splice variants have different enzymatic properties. J Biol Chem 2000;275:19018–24.
[15] Mulero JJ, Yeung G, Nelken ST, Ford JE. CD39-L4 is a secreted human apyrase, specific for the hydrolysis of nucleoside diphosphatases. J Biol Chem 1999;274:20064–7.
[16] Yeung G, Mulero JJ, McGowan DW, Bajwa SS, Ford JE. CD39L2, a gene encoding a human nucleoside diphosphatase, predominantly expressed in the heart. Biochemistry 2000;39:12916–23.
[17] Hicks-Berger CA, Chadwick BP, Frischauf AM, Kirley TL. Expression and characterization of soluble and membrane-bound human nucleoside triphosphate diphosphohydrolase 6 (CD39L2). J Biol Chem 2000;275:34041–5.
[18] Braun N, Fengler S, Ebeling C, Servos J, Zimmermann H. Sequencing, functional expression and characterization of rat NTPDase6, a nucleoside diphosphatase and novel member of the ecto-nucleoside triphosphate diphosphohydrolase family. Biochem J 2000;351:639–47.
[19] Shi JD, Kukar T, Wang CY, Li QZ, Cruz PE, Davoodi-Semiromi A, et al. Molecular cloning and characterization of a novel mammalian endo-apyrase (LALP1). J Biol Chem 2001;276:17474–8.

[20] Vollmayer P, Koch M, Braun N, Heine P, Servos J, Israr E, et al. Multiple ecto-nucleotidases in PC12 cells: identification and cellular distribution after heterologous expression. J Neurochem 2001;78: 1019–28.
[21] Smith TM, Kirley TL. Glycosylation is essential for functional expression of a human brain ecto-apyrase. Biochemistry 1999;38: 1509–16.
[22] Murphy DM, Kirley TL. Asparagine 81, an invariant glycosylation site near apyrase conserved region 1, is essential for full enzymatic activity of ecto-nucleoside triphosphate diphosphohydrolase 3. Arch Biochem Biophys 2003;413:107–15.
[23] Smith TM, Carl SAL, Kirley TL. Mutagenesis of two conserved tryptophan residues of the E-type ATPases: inactivation and conversion of an ecto-apyrase to an ecto-NTPase. Biochemistry 1999;38: 5849–57.
[24] Yang F, Hicks-Berger CA, Smith TM, Kirley TL. Site-directed mutagenesis of human nucleoside triphosphate diphosphohydrolase 3: the importance of residues in the apyrase conserved regions. Biochemistry 2001;40:3943–50.
[25] Kirley TL, Yang F, Ivanenkov VV. Site-directed mutagenesis of human nucleoside triphosphate diphosphohydrolase 3: the importance of conserved glycine residues and the identification of additional conserved protein motifs in eNTPDases. Arch Biochem Biophys 2001;395:94–102.
[26] Hicks-Berger CA, Yang F, Smith TM, Kirley TL. The importance of histidine residues in human ecto-nucleoside triphosphate diphosphohydrolase-3 as determined by site-directed mutagenesis. Biochim Biophys Acta 2001;1547:72–81.
[27] Smith TM, Kirley TL. Site-directed mutagenesis of a human brain ecto-apyrase: evidence that the E-type ATPases are related to the actin/heat shock 70/sugar kinase superfamily. Biochemistry 1999;38:321–8.
[28] Murphy DM, Ivanenkov VV, Kirley TL. Identification of cysteine residus res-ponsible for oxidative cross-linking and chemical inhibition of human nucleoside triphosphate diphosphohydrolase 3. J Biol Chem 2002;277:6162–9.
[29] Wang TF, Ou Y, Guidotti G. The transmembrane domains of ectoapyrase (CD39) affect its enzymatic activity and quaternary structure. J Biol Chem 1998;273:24814–21.
[30] Grinthal A, Guidotti G. Transmembrane domains confer different substrate specificities and adenosine diphosphate hydrolysis mechanisms on CD39, CD39L1, and chimeras. Biochemistry 2002;41:1947–56.
[31] Bradford MM. A rapid and sensitive method for quantification of microgram quantities of protein utilizing the principle of protein-dye binding. Anal Biochem 1976;72:248–54.
[32] Sévigny J, Lévesque FP, Grondin G, Beaudoin AR. Purification of the blood vessel ATP diphosphohydrolase, identification and localization by immunological techniques. Biochim Biophys Acta 1997;1334:73–88.
[33] Baykov AA, Evtushenko OA, Avaeva SM. A malachite green procedure for orthophosphate determination and its use in alkaline phosphatase-based enzyme immunoassay. Anal Biochem 1988;171:266–70.
[34] Kirley TL. Complementary DNA cloning and sequencing of the chicken muscle ecto-ATPase—homology with the lymphoid cell activation antigen CD39. J Biol Chem 1997;272:1076–81.
[35] Nagy AK, Knowles AF, Nagami GT. Molecular cloning of the chicken oviduct ecto-ATP-diphosphohydrolase. J Biol Chem 1998;273: 16043–9.
[36] Picher M, Sévigny J, D'Orleans-Juste P, Beaudoin AR. Hydrolysis of P2-purinoceptor agonists by a purified ectonucleotidase from the bovine aorta, the ATP-diphosphohydrolase. Biochem Pharmacol 1996;51:1453–60.
[37] Laliberté JF, Beaudoin AR. Sequential hydrolysis of the gamma- and beta-phosphate groups of ATP by the ATP diphosphohydrolase from pig pancreas. Biochim Biophys Acta 1983;742:9–15.
[38] Sévigny J, Sundberg C, Braun N, Guckelberger O, Csizmadia E, Qawi I, et al. Differential catalytic properties and vascular topography of murine nucleoside triphosphate diphosphohydrolase 1 (NTPDase1) and NTPDase2 have implications for thromboregulation. Blood 2002;99:2801–9.
[39] Kyte J, Doolittle RF. A simple method for displaying the hydropathic character of a protein. J Mol Biol 1982;157:105–32.